Response Letter

Ms. Ref. No.: egusphere-2026-1745

Title: High-frequency monitoring of SO_2 plumes from moderate-scale volcanic eruptions using a synergy of GEO and LEO satellites: A case study of the 2024 Kanlaon eruption

Atmospheric Chemistry and Physics

Our Response:

We thank the Editor and the two expert reviewers for their constructive comments, which have materially strengthened the rigor and presentation of the manuscript. We have made major and careful modifications to the original manuscript according to all the comments and suggestions from the reviewers.

The major changes include:

(1) Systematically expanded the uncertainty characterization of the GIIRS SO_2 retrieval. We added comprehensive sensitivity analyses in the main text (Section 4.2) and the Supplementary Materials to quantitatively evaluate the impacts of surface temperature variations, water vapor profile changes, and volcanic ash masking effects on retrieval performance. Detailed forward modeling of volcanic ash was also included in the supplement.

(2) Refined the theoretical details of the retrieval algorithm and model configurations. We restructured and expanded upon the specific details of the retrieval process: detailing the radiative transfer model (e.g., HITRAN database, and spectral resolution); clarifying the construction of the error covariance matrix (S_ε) and its representativeness of realistic environmental interferences; demonstrating the relationship between the spectral shape features of the Jacobian matrix (K) and varying SO_2 column densities through sensitivity tests; and clarifying the specific operational procedures for constraining the GIIRS SO_2 layer height using synergistic LEO satellite observations.

(3) Evaluated the operational detection threshold based on real observation scenarios. Building upon the theoretical detection limit, we incorporated a statistical evaluation of real SO_2-free background radiance pixels. The resulting empirical detection threshold (~4–6 DU at 10–15 km altitudes) inherently internalizes the impacts of realistic environmental interferences such as clouds and water vapor.

(4) Comprehensively revised inaccurate or absolute statements throughout the manuscript to enhance objectivity and rigor. We strictly reviewed the qualitative descriptions across the entire manuscript and corrected claims that lacked sufficient evidence. For example, we revised the inappropriate statements regarding the "global applicability" of the framework throughout the text, and discussed the physical limitations and application prerequisites when migrating this method to other environmental conditions.

Item-by-item responses to the specific comments are provided below. Modifications to the original manuscript are indicated by yellow highlights in the revised manuscript.

Response to Reviewer 1

General comments from reviewer 1:

This study integrates SO_2 plume height and column density retrieval from several GEO and LEO satellites to exhibit a case study of the 2024 Kanlaon eruption. The main innovation of this study is the weak v1 absorption band is leveraged to estimate SO_2 column density for FY-4B/GIIRS. The large differences between satellite retrievals and model simulations demonstrate the significance of the synergy of GEO and LEO satellites. Some comments should be addressed before the consideration of its publication.

Response to Reviewer 1's general comment

We sincerely thank the reviewer for taking the time to review our manuscript and for the positive overall assessment. We greatly appreciate your constructive comments, which are very helpful in improving the quality of this paper. We have carefully addressed all the specific comments and revised the manuscript accordingly. Please find our detailed point-by-point responses below.

Specific comments from reviewer 1:

R1-S1

1. Water vapor strongly absorbs radiation in both v1 and v3 band as shown Fig. 2. How does it affect the retrievals of SO_2 plume height and column density? Should water vapor profiles or water vapor column concentrations be determined prior to the retrieval of SO_2 plume height and column density?

Response:

We thank the reviewer for insightful comments. In our algorithmic framework, there is no need to separately determine or retrieve the water vapor profile prior to the SO_2 retrieval. Our retrieval algorithm can effectively overcome water vapor interference.

(1) Impact on SO_2 column density retrieval.

In our retrieval framework, water vapor fluctuations, along with other interfering factors such as cloud contamination and forward model errors, are encapsulated within the error covariance matrix ($\mathbf{S}_{\boldsymbol{\varepsilon}}$). The core of this retrieval method is based on fitting the SO_2 spectral shape. The spectral features described by the covariance matrix do not significantly affect the final SO_2 retrieval. Water vapor does not mask or distort the high-frequency SO_2 absorption spectral shape. In contrast, atmospheric effects that alter the SO_2 spectral signatures (such as clouds and volcanic ash located above the plume) weaken these spectral features and lead to underestimations in the retrieval **(Carboni et al., 2012)**.

Additionally, the presence of water vapor affects the true thermal contrast, which impacts the observation signal-to-noise ratio and the final retrieval. This impact is more pronounced for GIIRS due to its sole weak absorption band, whereas the impact on HIRAS is relatively minor. We have supplemented a sensitivity experiment in Section 4.2. By scaling the entire water vapor profile by factors ranging from 0.6 to 1.5 (in practice, we utilize ERA5 water vapor profiles, so the actual residual water vapor fluctuations are far less extreme), we observed that the impact of water vapor variations on the GIIRS SO_2 retrieval is limited. Taking an assumed 30 DU SO_2

plume as an example, when the water vapor scaling factor changes from 0.6 to 1.5, the relative error (underestimation) of the SO_2 retrieval only shifts from -28.0% to -30.7%, compared to -28.7% under the unperturbed condition (1.0x water vapor).

(2) Impact on SO_2 plume height estimation

The physical essence of the HRI method is to quantify the shape-matching degree between the observed spectra and the theoretical SO_2 spectral features. Interferences from unconstrained parameters in the atmosphere (including the natural presence and variation of water vapor) are already effectively accounted for in the background covariance matrix (**S**) constructed from real background observations. The presence of water vapor does not alter the relative shape of the SO_2 absorption cross-section across different altitudes. As long as this relative shape remains unchanged, HRI can accurately identify the altitude layer with the highest correlation (i.e., the peak-finding remains stable) **(Clarisse et al., 2026)**.

Updated Section 3.2:

"The resulting residual covariance matrix effectively encapsulates the combined influence of instrumental noise, forward model errors, observation geometries, and the variability of unresolved surface and atmospheric parameters (e.g., water vapor fluctuations, other interfering gases and clouds contamination) ..."

Updated Section 4.2:

"...At higher SO_2 concentrations, a negative deviation in actual water vapor yields better results by reducing lower-atmosphere continuum absorption and enhancing the true TC...";

"...Spectral signatures described by the covariance matrix (e.g., water vapor) have a limited impact on the SO_2 retrieval, primarily affecting the signal-to-noise ratio via TC... In contrast, coexisting volcanic ash can weaken the SO_2 spectral features... These results align with Carboni et al. (2012). Their study also included the impact of water clouds..."

Updated Fig. S2(b):

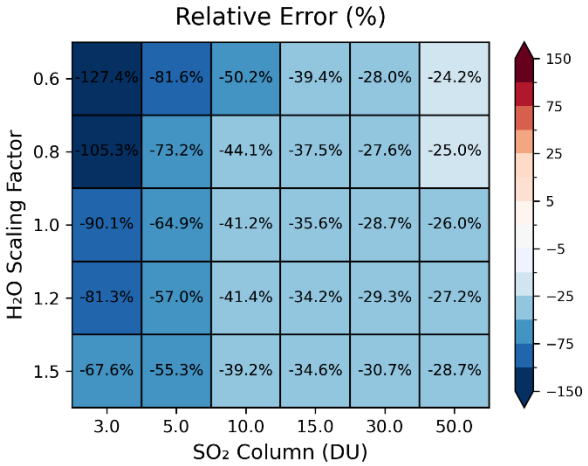


Fig. S2(b). Sensitivity analysis of the of FY-4B/GIIRS SO_2 retrievals under simulated environmental perturbations. Heatmaps show the retrieval relative errors induced by (b) scaled water vapor profiles (0.6 to 1.5).

R1-S2

2. Are the Jacobians in Sect. 3.1 sensitive to the variation in SO_2 columns. A constant SO_2 column density of 10 DU for each layer is used to while the true SO_2 column density could be quite different from the assumed constant. How does it affect the calculation HRI(h)? Will it lead to significant uncertainty of HRI(h), hence the plume height estimation?

Response:

Yes, the absolute magnitudes of the Jacobians ($\mathbf{K}_{\boldsymbol{h}}$) are highly sensitive to variations in SO_2 column densities, but the normalized Jacobians (i.e., their relative spectral shapes) are insensitive to column variations. The core mechanism of the $\mathbf{HRI}(\boldsymbol{h})$ algorithm is to match the relative spectral shape between the observed spectra and the theoretical Jacobians within a covariance-weighted space, rather than fitting absolute radiances. Therefore, using a constant 10 DU assumption does not introduce significant uncertainty to the $\mathbf{HRI}(\boldsymbol{h})$ calculation and the subsequent plume height estimation.

To demonstrate this, we conducted a simulation experiment by extracting approximately 200 observation points from potential volcanic plume regions in the HIRAS data on June 2, 2024. We calculated and averaged the Jacobians for several different SO_2 column densities (1, 10, 30, and 50 DU) across various altitude layers. Here, we present the results for the 5, 10, 15, and 20 km altitudes. As shown in Figure R1, it can be seen that while the changes in the absolute magnitudes of the Jacobians are quite obvious, the relative spectral shapes remain highly consistent within the same altitude layer. Changes in true concentration primarily result in a near-linear scaling of the Jacobian matrix, and the normalized spectral shapes exhibit no significant distortion across different concentrations. Notably, for the most prevalent weak plume observations (~1 DU) in this Kanlaon eruption, the spectral shape matches the 10 DU assumption well.

Comparing the results across different altitudes reveals that shape perturbations caused by concentration variations are much smaller than the spectral shape variations induced by altitude differences. Therefore, as long as the shape variations caused by concentration do not obscure the altitude-dependent spectral features, using the pre-calculated 10 DU Jacobians can capture the maximum shape correlation between the observed spectra and the theoretical model, and estimate accurate layer height.

Updated Section 3.1:

"Although the absolute magnitudes of $\mathbf{K}_{\boldsymbol{h}}$ scale with varying SO_2 loadings, sensitivity tests (not shown) indicate that their normalized spectral shapes remain highly similar for different SO_2 columns at a given altitude. Using a fixed 10 DU proxy should not influence the height estimation."

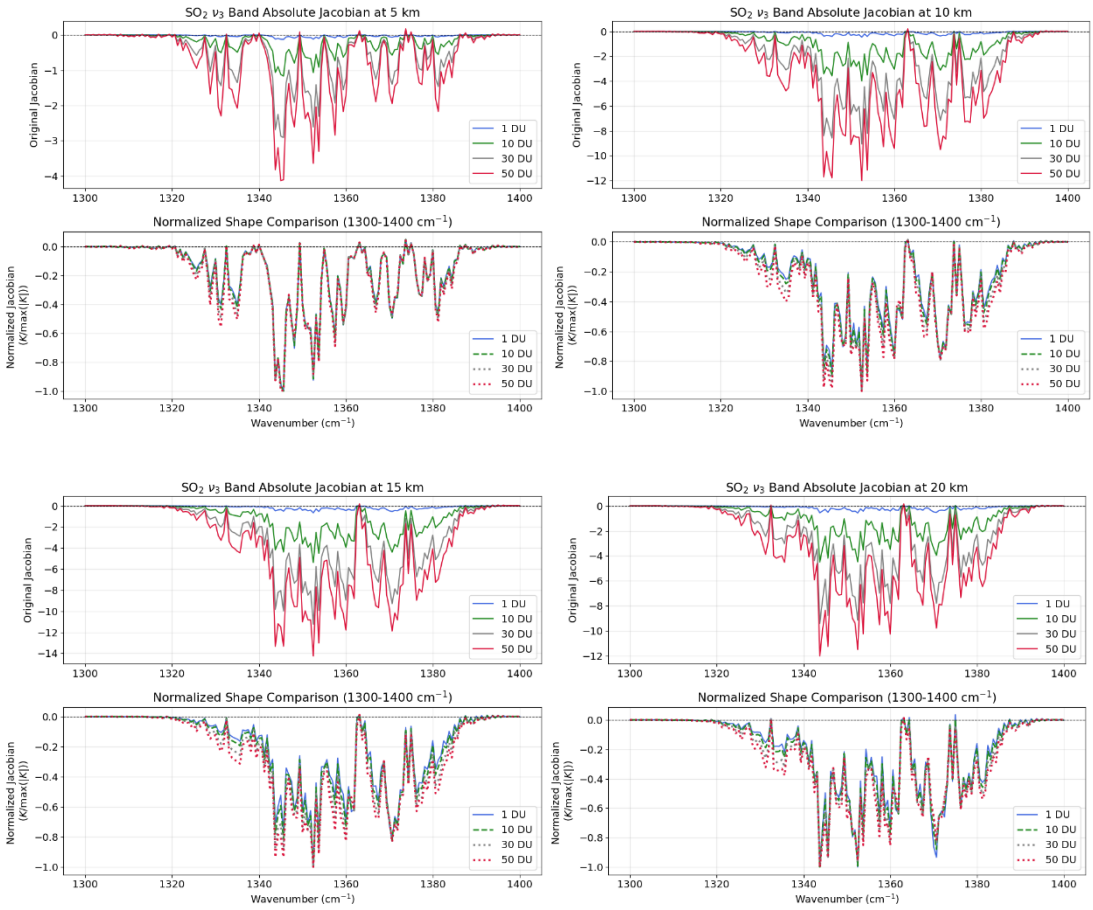


Fig. R1. Sensitivity of the absolute and normalized SO_2 $\nu 3$-band Jacobians to varying column densities (1,10,30, 50 DU) at different altitudes (5, 10, 15, 20 km).

R1-S3

3. More explanations are needed for "Notably, the SO_2 layer height for the FY-4B/GIIRS observations is constrained using the retrieval results from the synergistic HIRAS and CrIS." How are the retrieve results applied to retrieve SO_2 layer height for the FY-4B/GIIRS observations?

Response:

GIIRS lacks the strong $\nu 3$ band required for direct height retrieval, thus we utilized the synergistic LEO (HIRAS and CrIS) retrieval results. The specific procedure is as follows: for observations with concurrent LEO overpasses, the plume is divided into 1°–2° sub-regions, and the local representative heights (mean heights) from the LEO observations within each sub-region are assigned to the corresponding GIIRS pixels. For GIIRS observations lacking concurrent LEO overpasses, the heights are estimated via temporal interpolation along the plume transport trajectory. We have added these specific descriptions to the revised manuscript.

Updated Section 3.1:

"Notably, direct height retrieval from GIIRS spectra proved challenging due to its restricted spectral coverage, which only encompasses the weaker SO_2 $\nu 1$ band. To overcome this, the layer height for GIIRS is constrained using synergistic LEO retrievals

(HIRAS and CrIS). Specifically, the plume is divided into 1°–2° sub-regions, and the local averaged heights from concurrent LEO observations are assigned to the corresponding GIIRS pixels. For GIIRS observations lacking concurrent LEO overpasses, the heights are estimated via temporal interpolation along the plume trajectory."

R1-S4

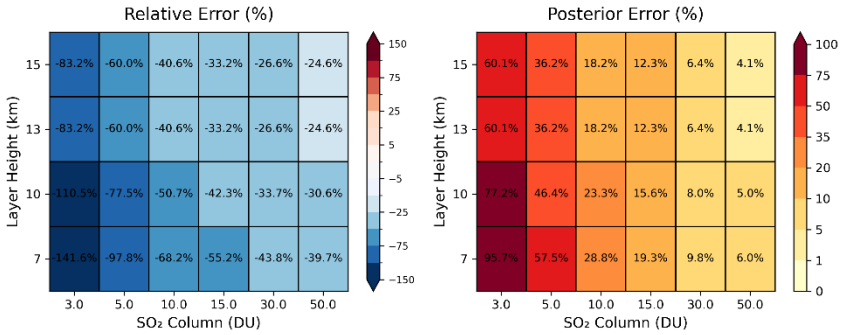
4. 3b and 3d are good. I suggest revising the vertical axis, with lower atmospheric levels at the bottom and upper levels at the top. This will avoid such misunderstanding when reader do not examine the figures carefully.

Response:

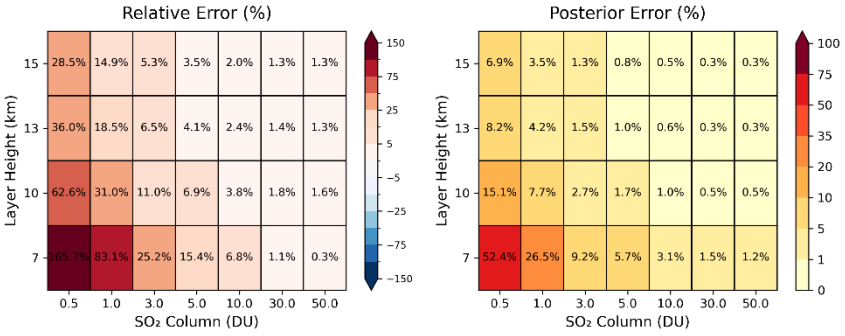
Changed as suggested.

Updated Fig. 3(b, d):

(b)



(d)



R1-S5

5. Line 50-59: All acronyms and abbreviations should be spelled out upon their first occurrence.

Response:

Changed as suggested.

Updated Section 1:

"The representative UV instruments include the Total Ozone Mapping Spectrometer (TOMS; e.g., Krueger, 1983), the Global Ozone Monitoring Experiment (GOME; e.g., Eisinger & Burrows, 1998), the Scanning Imaging Absorption Spectrometer for Atmospheric Chartography (SCIAMACHY; e.g., Lee et al., 2008), the Ozone Monitoring

Instrument (OMI; e.g., Krotkov et al., 2006; Theys et al., 2015), the second-generation Global Ozone Monitoring Experiment (GOME-2; e.g., Rix et al., 2012), the Ozone Mapping and Profiler Suite (OMPS; e.g., Yang et al., 2013), and the TROPOspheric Monitoring Instrument (TROPOMI; e.g., Queißer et al., 2019; Theys et al., 2017). In the infrared, these sounders include the Moderate Resolution Imaging Spectroradiometer (MODIS; e.g., Corradini et al., 2009), the Advanced Spaceborne Thermal Emission and Reflection Radiometer (ASTER; e.g., Urai, 2004), the Atmospheric Infrared Sounder (AIRS; e.g., Carn et al., 2005), the Tropospheric Emission Spectrometer (TES; e.g., Clerbaux et al., 2008), the Infrared Atmospheric Sounding Interferometer (IASI; e.g., Carboni et al., 2012; Clarisse et al., 2008; Walker et al., 2012), the Cross-track Infrared Sounder (CrIS; Hyman & Pavolonis, 2020), and the Hyperspectral Infrared Atmospheric Sounder (HIRAS; Li et al., 2025; Zeng et al., 2025). Additionally, volcanic SO2 can also be retrieved from microwave band measurements, such as the Microwave Limb Sounder (MLS; e.g., Pumphrey et al., 2015).”

R1-S6

6. The subscript 2 in SO_2 is often missing in many places.

Response:

We thank the reviewer for pointing this out. We have carefully checked the entire manuscript and corrected all instances where the subscript 2 in was missing.

References:

Carboni, E., Grainger, R., Walker, J., Dudhia, A., and Siddans, R.: A new scheme for sulphur dioxide retrieval from IASI measurements: Application to the Eyjafjallajökull eruption of April and May 2010, Atmospheric Chemistry and Physics, 12, 11417–11434, https://doi.org/10.5194/acp-12-11417-2012, 2012.

Clarisse, L., Franco, B., Fabris, L., Theys, N., Hadji-Lazaro, J., Hurtmans, D., Clerbaux, C., and Coheur, P.-F.: A 19-year record of atmospheric sulphur dioxide (SO2) derived from IASI measurements, Earth System Science Data, 18, 6667–6706, https://doi.org/10.5194/essd-18-6667-2026, 2026.

Response to Reviewer 2

General comments from reviewer 2:

This manuscript presents a comprehensive synergistic satellite observation framework for monitoring volcanic SO_2 emissions by integrating geostationary hyperspectral infrared observations from FY-4B/GIIRS and GEMS with polar-orbiting satellite observations from HIRAS, CrIS, IASI, TROPOMI, and MLS. Using the June 2024 eruption of Mt. Kanlaon in the Philippines as a case study, the authors demonstrate the potential of combining high-temporal-resolution geostationary observations with highly sensitive low-Earth-orbit (LEO) measurements to characterize the three-dimensional evolution and atmospheric lifetime of volcanic SO_2 plumes.

The manuscript is generally well structured, and the multi-sensor comparisons provide an interesting perspective on the complementary capabilities of geostationary and polar-orbiting observations. However, several aspects related to retrieval uncertainty characterization, validation strategy, and interpretation of the results require further clarification and improvement before the conclusions can be fully supported.

Therefore, I recommend major revision before the manuscript can be considered for publication.

Response to Reviewer 2's general comment

We sincerely thank the reviewer for taking the time to review our manuscript and for the positive overall assessment of our synergistic observation framework. We greatly appreciate your constructive comments regarding retrieval uncertainty characterization, validation strategy, and interpretation of the results, which are very helpful in improving the quality of this paper. We have carefully addressed all the specific comments and revised the manuscript accordingly. Please find our detailed point-by-point responses below.

Major comments:

R2-M1

1. The uncertainty characterization of the GIIRS SO_2 retrieval requires further improvement.

The retrieval algorithm is based on an optimal estimation framework, in which unresolved atmospheric effects are incorporated into the measurement error covariance matrix S_ε. Although this approach is theoretically reasonable, the current construction of S_ε appears to rely mainly on SO_2-free background scenes.

However, volcanic plume environments differ substantially from background atmospheric conditions, particularly due to:

(1) enhanced water vapor variability; (2) volcanic ash loading; (3) cloud contamination; (4) complex thermal and radiative conditions.

Therefore, the assumption that background residual statistics can fully represent uncertainties under volcanic plume conditions may not always be valid.

The authors should clarify: (1) How representative are the selected SO_2-free regions for actual volcanic plume environments? (2) Does S_ε vary with atmospheric conditions, observation geometry, or surface characteristics? (3) What are the potential impacts of systematic biases that cannot be adequately represented by the covariance matrix?

A sensitivity analysis under different atmospheric conditions would significantly

strengthen the uncertainty assessment.

Response:

We thank the reviewer for this constructive comment. Our responses to your questions are detailed below:

(A) Representativeness of S_ε.

In our algorithm, S_ε possesses adequate spatiotemporal representativeness. The samples used to construct S_ε were extracted from real observations acquired on the day prior to the eruption (June 2, 2024), which spatially fully covered the potential retrieval region. This ensures that the background statistical properties encapsulate the actual observation geometries, surface characteristics (e.g., emissivity differences between land and ocean), and natural fluctuations of the background atmosphere, specifically including meteorological clouds.

Under volcanic eruption conditions, the variability of water vapor and clouds can be relatively large. However, because the real observations used to construct S_ε already account for meteorological clouds, and clouds inherently contain abundant water vapor, such variations in water vapor and clouds are essentially covered by S_ε. Furthermore, since surface temperature is jointly retrieved with SO_2 in our algorithm, the absolute variations of thermal radiation in the actual environment are directly compensated for by the retrieval process, eliminating the need to include them in S_ε. Overall, with the exception of the potentially co-existing thick volcanic ash in a real eruption environment (which is not included in S_ε), S_ε encompasses most natural variability, including clouds, making it representative of the actual volcanic eruption environment.

(B) Does S_ε vary with conditions?

No, S_ε does not vary with atmospheric conditions, observation geometries, or surface characteristics. In our algorithm implementation, S_ε is custom-built for a specific retrieval task (i.e., a specific target region and an adjacent time window). It intrinsically contains the statistical variance of the local observation geometries and surface features, but remains a single, fixed matrix throughout the entire retrieval process for this event.

(C) Systematic biases not adequately represented by the covariance matrix.

The primary unmodeled factor not included or described in the covariance matrix is volcanic ash. The presence of volcanic ash causes broadband physical masking that diminishes the SO_2 spectral features, subsequently leading to a systematic underestimation in the SO_2 retrieval **(Carboni et al., 2012)**.

(D) Sensitivity analysis under different atmospheric conditions

We have systematically conducted a sensitivity analysis in Section 4.2 of the revised manuscript (adding Fig. S2) to quantitatively evaluate the interferences of surface temperature, water vapor, and volcanic ash on the GIIRS SO_2 retrievals.

(D1) Surface Temperature (ST): In the sensitivity experiment, we perturbed the true surface temperature of the synthetic spectra (-10 K to +10 K). The results show that a higher true surface temperature yields better retrieval performance. (For example, taking a 30 DU plume as an assumption, as the temperature increases from -10 K to +10 K, the retrieval underestimation error narrows from -32.5% to -24.4%). This is primarily because an increase in temperature enhances the thermal contrast, which directly improves the observation signal-to-noise ratio. Because ST is jointly solved iteratively during the actual retrieval, the algorithm has the

capability to self-adapt to temperature variations in the real environment. Temperature anomalies in the real environment will not introduce obvious systematic errors to the retrieval.

(D2) Water Vapor: We scaled the ERA5 water vapor profiles by factors ranging from 0.6 to 1.5 (water vapor does not participate in the retrieval iterations and remains fixed at the prior). The results indicate that the overall impact of water vapor variations on the GIIRS SO_2 retrieval is limited. Taking a 30 DU assumption as an example, when the water vapor scaling factor changes from 0.6 to 1.5, the underestimation of the SO_2 retrieval merely shifts from -28.0% to -30.7% (the error is -28.7% at 1.0x water vapor). An increase in water vapor enhances lower-level absorption, which consequently weakens the thermal contrast and degrades the retrieval.

(D3) Volcanic Ash: We simulated volcanic ash at varying altitudes (2–12 km) and optical depths (AOD 0.1–1.0). The results demonstrate that when ash is located below the SO_2 layer, it acts as a colder radiative background, weakening the thermal contrast and thereby affecting the retrieval. Conversely, when ash is co-located with or above the plume, it generates a strong physical masking effect (e.g., according to the Beer-Lambert law, volcanic ash with AODs of 0.1 and 0.5 at 10 μm attenuates the underlying gas signal by 9.5% and 39.3%, respectively). This broadband attenuation directly diminishes the SO_2 spectral features, leading to severe underestimations. Detailed forward modeling of volcanic ash is provided in R2-M3.

In summary, our algorithm primarily relies on fitting the SO_2 spectral shape. The spectral impacts encapsulated within S_ε have a limited influence on the GIIRS SO_2 retrieval. For atmospheric physical variables, as long as they do not distort the SO_2 spectral signatures, their impacts on the retrieval are predominantly manifested through altering the thermal contrast and signal-to-noise ratio. In contrast, masking objects such as volcanic ash weaken the spectral signatures, causing an underestimation of SO_2, which aligns with the conclusions in **Carboni et al. (2012)**. Similar to volcanic ash, when water clouds are mixed with or above the plume, their strong broadband physical masking effect also leads to severe underestimations. The specific, practical impacts of clouds on the retrievals are discussed in more detail in our response to R2-M3 (combined with the Ruang volcano HRI results).

Updated Section 3.2:

"The resulting residual covariance matrix effectively encapsulates the combined influence of instrumental noise, forward model errors, observation geometries, and the variability of unresolved surface and atmospheric parameters (e.g., water vapor fluctuations, other interfering gases and clouds contamination) ..."

Updated Section 4.2:

4.2 Sensitivity of GIIRS retrievals to environmental interferences

To evaluate the algorithm's robustness against realistic physical anomalies and unmodeled volcanic ash, a sensitivity analysis is conducted for the GIIRS retrievals. First, to simulate environmental perturbations, synthetic "true" spectra are generated by scaling the entire ERA5 water vapor profile by factors ranging from 0.6 to 1.5, and by shifting the surface temperature (ST) from -10 K to +10 K in 5 K increments. In this scenario, the SO_2 layer is fixed at 13 km with column densities ranging from 3 to 50 DU. We utilize unperturbed background priors during the retrieval process. Notably, ST is jointly retrieved within the optimal estimation framework, whereas the water vapor profile remains fixed. Secondly, to assess the radiative masking effect of co-emitted

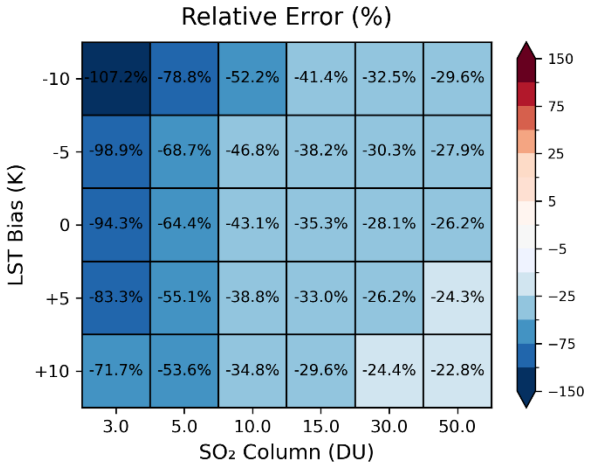
volcanic ash, the complex refractive index of Aso ash from the Aerosol Refractive Index Archive (ARIA).is incorporated (Reed et al., 2018). Aso is selected as a proxy due to its highly analogous subduction-zone setting and andesitic magma composition. In this experiment, the SO_2 layer is fixed at an altitude of 10 km with a column density of 30 DU. Ash layers with infrared aerosol optical depths (AOD at 10 μm) ranging from 0.1 to 1.0 are introduced at varying altitudes between 2 and 12 km (detailed ash forward modeling configurations are provided in Text S2).

Based on 500 sampling points extracted at equal intervals from the potential plume region observed by GIIRS on June 2, sensitivity experiments are conducted. The relative error distributions of the retrieval results are shown in Fig. S2. Fig. S2a shows that the retrieval accuracy for all SO_2 column loadings increases with ST. This is because an increase in ST significantly improves the thermal contrast (TC) between the surface and the SO_2 plume, enhancing the signal-to-noise ratio and thereby improving the retrieval performance. Fig. S2b illustrates the impact of water vapor profile mismatches. At higher SO_2 concentrations, a negative deviation in actual water vapor yields better results by reducing lower-atmosphere continuum absorption and enhancing the true TC. However, at extremely low SO_2 concentrations, this profile mismatch dominates the error. Since the prior remains fixed, a negative deviation introduces unmodeled baseline radiance. To minimize residuals, the algorithm compensates by retrieving negative SO_2 values, elevating the detection threshold. Fig. S2c illustrates the impact of volcanic ash at different altitudes and AODs. When ash is located below the SO_2 plume, it acts as the radiation background; the closer it is to the SO_2 layer, the lower the background temperature, which weakens the TC and degrades the retrieval. In contrast, ash co-located with or above the SO_2 plume physically masks the spectral effect. According to the Beer-Lambert law, volcanic ash with an AOD of 0.1 or 0.5 at 10 μm attenuates the underlying gas signal by approximately 9.5% and 39.3%, respectively. This broadband attenuation diminishes the SO_2 spectral features, leading to severe underestimations, making near-threshold SO_2 signals highly susceptible to missed detections.

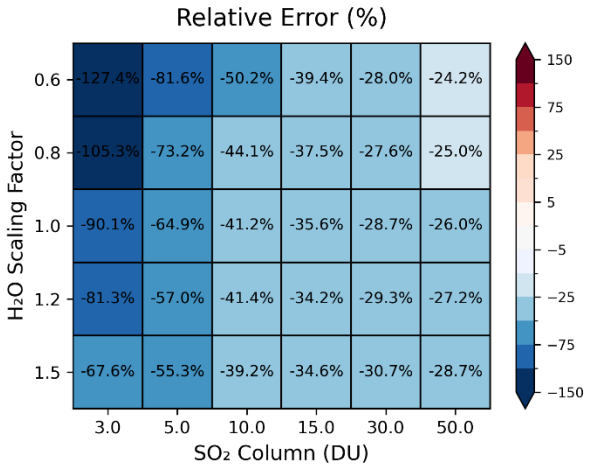
In summary, the core of this retrieval method is based on fitting the SO_2 spectral shape. Spectral signatures described by the covariance matrix (e.g., ST and water vapor) have a limited impact on the SO_2 retrieval, primarily affecting the signal-to-noise ratio via TC and generally causing conservative underestimations. However, volcanic ash can weaken the SO_2 spectral features and cause a significant underestimation of the total column when co-located with or above the plume. These results align with Carboni et al. (2012). Their study also included the impact of water clouds. Similar to volcanic ash, when water clouds are mixed with or above the SO_2 plume, their strong broadband masking effect leads to severe underestimation, whereas underlying clouds or aerosol located have small impact. Developing simultaneous retrieval algorithms for SO_2, ash, and clouds remains a key future direction."

Updated Fig. S2:

(a)



(b)



(c)

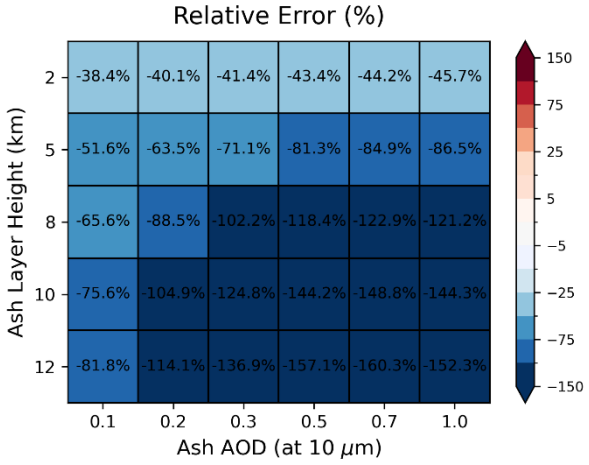


Figure S2. Sensitivity analysis of the of FY-4B/GIIRS SO_2 retrievals under simulated environmental perturbations. Heatmaps show the retrieval relative errors induced by (a) surface temperature variations (-10 K to +10 K), (b) scaled water vapor profiles (0.6 to 1.5), and (c) volcanic ash layer height (2 to 12 km) as a function of infrared ash aerosol optical depth (AOD) at 10 μm for a fixed SO_2 plume (30 DU at 10 km altitude).

R2-M2

2. The influence of limited GIIRS spectral coverage on SO_2 sensitivity should be discussed more

quantitatively

The manuscript demonstrates that GIIRS can successfully detect high-concentration SO_2 plumes but has limited sensitivity to weak signals. Simulation experiments indicate that GIIRS generally underestimates SO_2 total columns, particularly under low-concentration conditions. However, the manuscript should provide a more quantitative discussion regarding: (1) the minimum detectable SO_2 column under realistic atmospheric conditions; (2) the dependence of detection capability on plume altitude; (3) the effects of surface temperature and atmospheric water vapor.

The reported theoretical detection limit (~3 DU under ideal conditions) may represent an optimistic lower bound. The authors should clarify how this threshold changes when realistic cloud effects, aerosol impacts, and forward-model uncertainties are considered.

Response:

We thank the reviewer for pointing this out. Our responses are as follows:

(A&B) Operational detection threshold under realistic atmospheric conditions and its altitude dependence

We have added a statistical evaluation based on real observations to illustrate the operational detection threshold under realistic atmospheric conditions. Specifically, we uniformly sampled approximately 15,000 SO_2-free real background pixels within the potential plume region prior to the eruption (1h to 10h UTC on June 3) and performed the full retrieval procedure on these pixels. These real background pixels naturally contain actual cloud contamination, water vapor perturbations, and forward model errors. The statistical results indicate that assuming plume heights of 15 km and 10 km, the means of the background retrievals are both near zero (0.06 DU), but the standard deviations (σ) reach ~2 DU and ~3 DU, respectively. Therefore, based on these real observations, we establish the empirical 2σ operational detection limits at ~4 DU (15 km) and ~6 DU (10 km). This result already encompasses the impacts of multiple interfering factors such as clouds and water vapor.

Furthermore, this also quantitatively reflects the phenomenon that as the altitude decreases, the detection limit increases from ~4 DU to ~6 DU. This is because the reduced thermal contrast in the lower atmosphere significantly decreases the observation signal-to-noise ratio at lower altitudes, thereby degrading the detection capability.

Additionally, some anomalously high retrieval values observed in the background areas are primarily attributed to systematic instrumental noise (which manifests as regularly arranged high-HRI pixels in Fig. 4). Because these false-positive signals are spatially isolated and scattered, they can be effectively eliminated based on the spatial coherence of the actual volcanic plume in practical applications.

(C) Effects of surface temperature, water vapor, and volcanic ash on the detection threshold

The impacts of these environmental variables on the SO_2 retrievals have been detailed in our response to comment R2-M1. Here, we focus on describing their impacts on the detection threshold:

(C1) Surface Temperature (ST): The ST primarily affects the retrieval performance by influencing the thermal contrast. A higher thermal contrast yields a lower actual detection threshold, and vice versa. Because ST is a solved variable in the retrieval, variations in ST under realistic environments will not introduce additional errors to the retrieval.

(C2) Water vapor is not a retrieved variable in our algorithm and is instead encapsulated

within S_ϵ using a fixed prior. For weak plumes near the detection limit (e.g., 3.0 DU), a negative deviation in the actual water vapor (e.g., 0.6x scaling) relative to the prior induces relative errors and elevates the actual detection threshold.

(C3) Thick clouds or volcanic ash produce strong broadband physical masking in realistic environments. For example, volcanic ash with an AOD of 0.5 causes approximately 39.3% signal attenuation. Such severe attenuation can easily suppress genuine SO_2 signals below the empirical detection limits (~4–6 DU) and cause missed detections, particularly for weak signals near the threshold. (Detailed discussions on cloud impacts are provided in our response to R2-M3).

Updated Section 5.2.1:

"Furthermore, to determine the operational detection threshold under realistic atmospheric conditions, a statistical evaluation of SO_2-free background observations is conducted. Specifically, approximately 15,000 SO_2-free pixels are uniformly sampled based on spatial distribution from five GIIRS scenes acquired prior to the eruption (1h to 10h UTC on June 3) within the potential plume region (70°–140°E, 0°–20°N). Assuming SO2 heights of 15 km and 10 km, both background retrievals yield a near-zero mean (0.06 DU), with standard deviations (σ) of ~2 DU and ~3 DU, respectively. Consequently, the empirical 2σ detection limits are established at ~4 DU (15 km) and ~6 DU (10 km), reflecting the reduced thermal contrast and signal-to-noise ratio at lower altitudes. These empirical thresholds inherently encompass realistic interferences such as clouds and water vapor. The anomalous high retrieval values observed in these background areas are likely attributed to systematic instrumental noise (which manifests as regularly arranged high-HRI pixels in Fig. 4). Because these false positives are spatially isolated, they can be effectively eliminated based on the spatial coherence of the actual volcanic plume."

Updated Section 4.2.:

"...Since the prior remains fixed, a negative deviation introduces unmodeled baseline radiance. To minimize residuals, the algorithm compensates by retrieving negative SO_2 values, elevating the detection threshold ..."

"...In contrast, ash co-located with or above the SO_2 plume physically masks the spectral effect.... This broadband attenuation diminishes the SO_2 spectral features, leading to severe underestimations, making near-threshold SO_2 signals highly susceptible to missed detections. ..."

R2-M3

3. The impacts of clouds and volcanic ash require more explicit consideration

The manuscript acknowledges that cloud and volcanic ash effects are not explicitly treated in the retrieval framework. However, these effects are particularly important for infrared SO_2 retrievals because volcanic eruptions usually generate SO_2, volcanic ash, and clouds simultaneously.

The authors should discuss: (1) Whether pixels affected by volcanic ash or clouds were excluded during retrieval; (2) How thin clouds influence the retrieved SO_2 total columns; (3)

Whether ash-related radiative effects could potentially be misinterpreted as SO_2 signals.

The current retrieval framework may underestimate uncertainties under realistic eruption conditions.

Response:

To explain the impacts of clouds and volcanic ash on GIIRS SO_2 retrievals, we conducted two parts of work:

(A) Volcanic ash forward simulation experiments (detailed in the Text S2 and Fig. S3)

First, we adopted the complex refractive index of real volcanic ash and assumed the particles to be volume-equivalent spheres with a lognormal size distribution (physical density of 2.5 g/cm^3). We calculated their mass extinction coefficient (MEC) and single scattering albedo (SSA) using Mie scattering theory. Referring to the measured results of similar volcanic ash samples by **Reed et al. (2018)**, we selected an effective radius r_{eff} = 0.6 μm in the final simulations. The calculation results demonstrate that within the GIIRS SO_2 absorption band (1000–1131.25 cm^{-1}), the SSA of volcanic ash at this particle size is extremely small (below 0.1), indicating that its extinction in this band is almost entirely dominated by absorption, with minor scattering.

Based on this, we fixed a 30 DU SO_2 plume at an altitude of 10 km and introduced volcanic ash with an infrared aerosol optical depth (AOD) of 0.2 at 10 μm at altitudes of 2 km, 10 km, and 12 km, respectively, to conduct forward spectral simulations and residual analyses. The results demonstrate that when volcanic ash is located below the SO_2 plume (e.g., at 2 km), it acts as an elevated thermal radiation background. Although it cools the background, it still preserves a sufficient thermal contrast with the colder SO_2 layer at 10 km, keeping the SO_2 spectral absorption features largely intact. Conversely, when volcanic ash is co-located with (10 km) or above (12 km) the plume, it strongly absorbs the underlying radiation, producing a pronounced broadband masking effect. This masking substantially flattens the SO_2 absorption lines, directly leading to severe systematic underestimations in our retrieval algorithm, which relies heavily on fitting these fine spectral signatures.

Finally, the specific quantitative impacts of volcanic ash at different altitudes and varying AODs on the SO_2 retrieval errors and detection thresholds have been detailed in our previous responses to comments R2-M1 and R2-M2.

(B) Evaluation of cloud interference based on the 2024 Ruang volcano observations

To illustrate the impact of clouds on SO_2 retrievals, we selected the Ruang volcano eruption in mid-April 2024 as a case study. The scale of this eruption is much larger than that of Kanlaon, making it more suitable for analyzing cloud interference. However, limited by the observation field of view, GIIRS only covered a partial region of the plume.

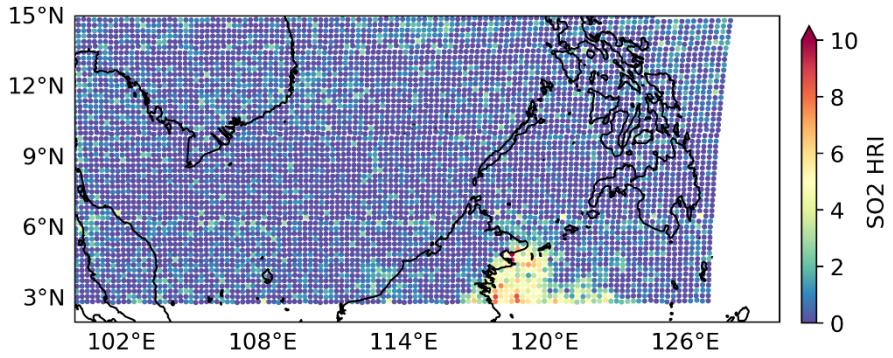
Figures R2a and R2b display the GIIRS SO_2 HRI and the GIIRS brightness temperature (BT) at the 900 cm^{-1} band (used for cloud identification and classification), respectively, at 01–02h UTC on April 18, 2024. In the bottom right corner of the observation region, a spatial coexistence of the high-concentration SO_2 plume (high HRI region) and a large-scale cold cloud region (low BT region) can be clearly observed. For quantitative analysis, Figure R2c further presents the co-located statistical results of the pixel-by-pixel SO_2 HRI and BT. The right panel is the scatter statistical plot, and the left panel is the corresponding classified spatial distribution map. We classified and evaluated the clouds using BT thresholds: (a) Thick/high cloud region

(BT < 250 K): This corresponds to the black squares in the left panel. The right scatter plot shows that the strong physical masking in this region largely truncates the underlying signals, and the HRI of all pixels is less than 2. Therefore, thick clouds can cause missed detections of SO_2 signals. (b) Thin/low cloud region (250 K < BT < 280 K): This corresponds to the purple circles in the left panel (the pink shaded area in the right panel). Statistics indicate that despite the presence of cloud interference (which weakens the SO_2 spectral signatures and causes retrieval underestimations), a large number of pixels within this range still extract significant SO_2 signals with HRI > 2.

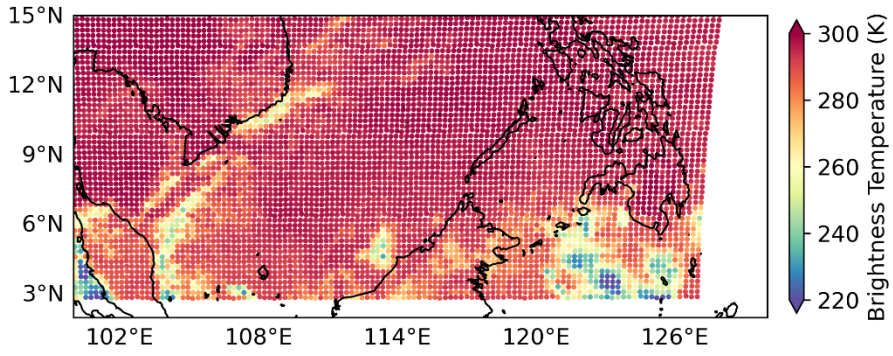
Overall, results indicate that thick clouds directly lead to severe missed detections of SO_2 signals, while thin clouds primarily result in underestimations of retrieval concentrations. The algorithm still exhibits penetration capabilities under thin cloud conditions. Therefore, we retained the cloud-affected pixels in our processing to maximize the continuity of the plume.

It should be noted that the specific empirical evaluation of cloud interference at the Ruang volcano mentioned above is provided here solely as a detailed response to you and has not been added to the revised manuscript. This is because **Carboni et al. (2012)** have already simulated clouds and their impacts on SO_2 retrievals, and there is no need for repeated demonstration in this paper.

(a)



(b)



(c)

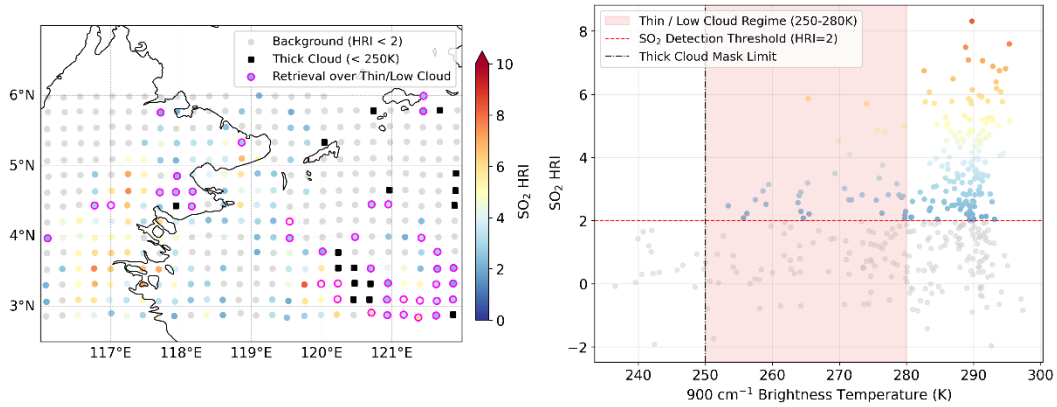


Fig. R2. Evaluation of cloud interference during the Ruang volcano eruption. Spatial distributions of (a) GIIRS SO_2 HRI and (b) 900 cm^{-1} brightness temperature (BT) observed on April 18, 2024. (c) Scatter plot of SO_2 HRI versus BT (right) and the corresponding classification map (left). Black squares indicate thick clouds (BT < 250 K), purple circles/pink shading indicate thin clouds (250–280 K), and the red dashed line is the HRI = 2 threshold.

Combining the above work, we answer your questions:

(1) We did not exclude pixels affected by volcanic ash or clouds. As demonstrated by our experimental results, the algorithm is capable of extracting valid signals from the interference of thin clouds and volcanic ash (although this interference will cause underestimations of SO_2). Direct masking would lose these valuable plume structures and concentration information.

(2) Similar to volcanic ash, thin clouds cause broadband signal attenuation that weakens the SO_2 spectral shape signatures, leading to a systematic and conservative underestimation of the retrieved SO_2 column concentrations. However, the algorithm can still extract the true SO_2 plume distribution shape from thin clouds.

(3) The radiative effects of volcanic ash will not be misinterpreted as SO_2 signals. Experimental results show that volcanic ash only causes true signals to be underestimated (missed detections), and it will never generate false positives (misinterpretations). The retrieval algorithm highly relies on fitting the unique high-frequency fine absorption line features of SO_2 molecules. Our Mie scattering simulations have confirmed that volcanic ash exhibits smooth broadband continuum extinction within the absorption band. It only alters the spectral baseline and weakens the gas absorption depth, making it mathematically and logically impossible to fabricate the high-frequency fine features of SO_2.

Updated Text S2:

"Text S2: Parameterization and simulations of volcanic ash in the forward model

To investigate the impact of volcanic ash on GIIRS SO_2 retrievals, volcanic ash aerosols are introduced into the forward radiative transfer model to conduct spectral simulation experiments. Fig. S3 illustrates the optical parameterization of volcanic ash and its impact on the simulated spectra. First, Fig. S3(a) shows the real and imaginary parts of the complex refractive index of volcanic ash used in the forward simulations. To calculate the volume extinction of volcanic ash, a lognormal size distribution is adopted in the simulation (the integrated reference number concentration N_0 is set to 3×10^5 cm^{-3}), expressed as:

$$n(r) = \frac{N_0 e^{-\frac{1}{2}\left(\frac{\ln(r)-\ln(r_m)}{\ln(s)}\right)^2}}{\sqrt{2\pi}\ln(s) r} \quad (1)$$

where r_m is the median radius and s is the geometric standard deviation. The conversion between the median radius r_m and the effective radius r_{eff} is given by:

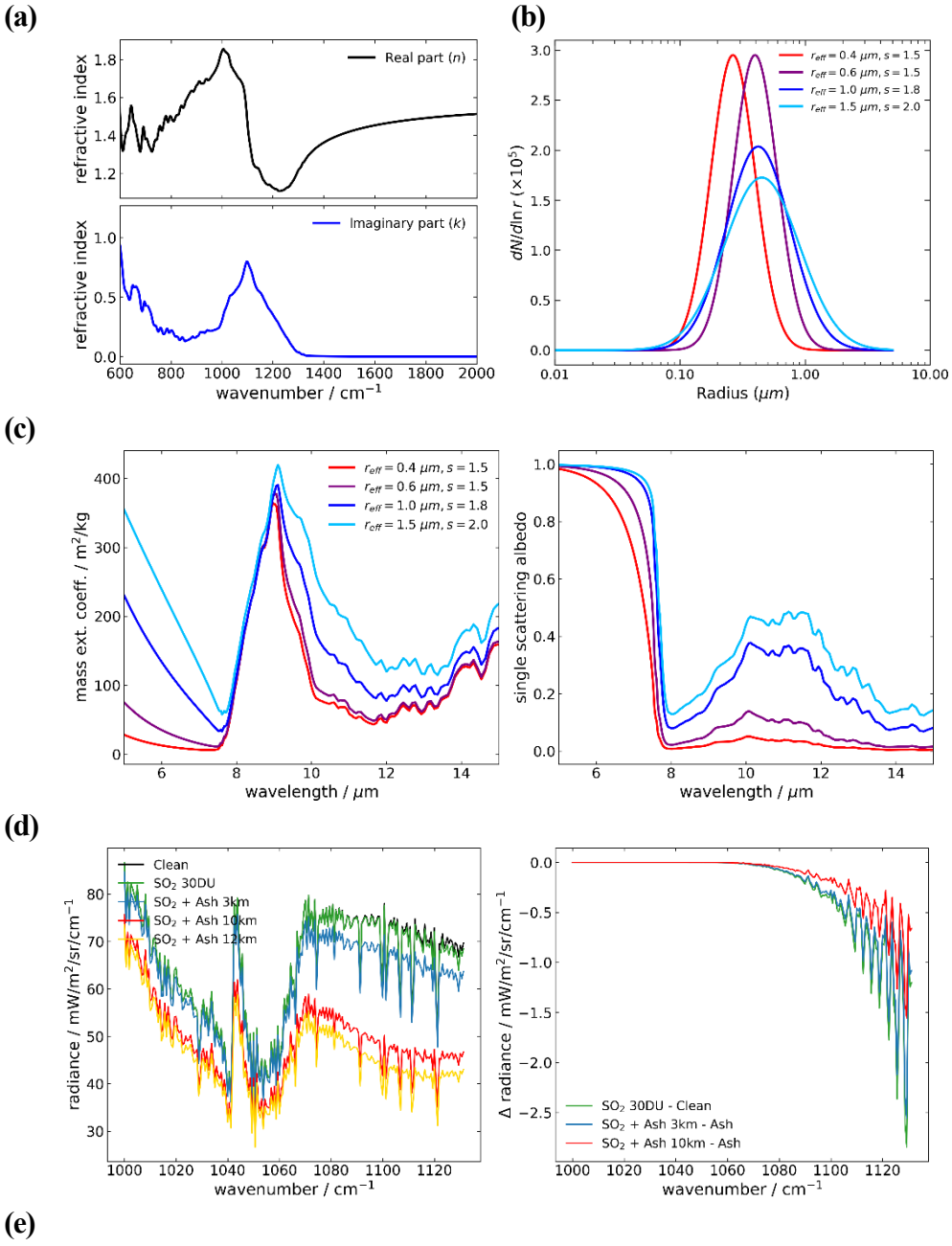
$$r_{eff} = r_m e^{(2.5(\ln(s))^2)} \quad (2)$$

To evaluate the impact of different particle sizes on the optical properties, multiple sets of effective radii and geometric standard deviations are configured, with their corresponding size distribution curves shown in Fig. S3(b). Based on the aforementioned complex refractive index and size distribution, and assuming volcanic ash particles are volume-equivalent spheres (with a physical density of 2.5 g/cm^3), we calculate the mass extinction coefficient (MEC) and single scattering albedo (SSA) under corresponding parameters using Mie scattering theory, as shown in Fig. S3(c). These calculated results are consistent with the simulated thermal infrared optical properties of volcanic ash presented by Piontek et al. (2021). For the interference analysis of the SO_2 retrieval for the Kanlaon volcanic eruption, the parameter set of r_{eff} = 0.6 μm is selected for the final forward simulations. This selection refers to the measured results of similar volcanic ash samples by Reed et al. (2018) (e.g., the measured r_{eff} = 0.574 μm for the Aso sample). As shown in the right panel of Fig. S3(c), under the selected particle size, the SSA is extremely small (below 0.1) within the GIIRS SO_2 absorption band (1000 to 1131.25 cm^{-1}). This indicates that the extinction of volcanic ash in this band is almost entirely dominated by absorption. Therefore, only the absorption cross-section of volcanic ash is considered in the forward radiative transfer model, ignoring its scattering effect.

Fig. S3(d) details the direct impact on the simulated top-of-atmosphere spectra after introducing volcanic ash at different altitudes in the forward model. In this set of simulations, the altitude of SO_2 is fixed at 10 km with a column amount of 30 DU; the infrared aerosol optical depth (AOD) of volcanic ash is uniformly set to 0.2 at 10 μm, and the ash layers are placed at altitudes of 3 km, 10 km, and 12 km, respectively. The left panel of Fig. S3(d) displays the simulated spectra containing aerosols, and the right panel shows the residuals (Δ radiance) between different spectra. The interference mechanism of volcanic ash can be clearly identified from the residual results: when volcanic ash is located at 3 km (well below the SO_2 plume), the aerosol primarily acts as the underlying thermal radiation background, maintaining a sufficient thermal contrast with the cold SO_2 layer at 10 km. Therefore, the shape of the SO_2 spectral absorption features is preserved, resulting in small spectral residuals. In contrast, when volcanic ash is located at 10 km (co-located with SO_2) or 12 km (above SO_2), the aerosols strongly absorb the upward radiation from below, producing a significant broadband masking effect. This causes the depth of the observed SO_2 absorption lines to be substantially weakened and the spectral shape features to be altered. Since this retrieval algorithm relies on fitting the SO_2 spectral absorption shape, such signal attenuation caused by co-located or overlying volcanic ash directly leads to severe underestimations in the retrieval results."

To further evaluate the uncertainty introduced by the absorption-only approximation, we compared our FY-GeoAIR model simulations with the Scattering Reference Forward Model (SRFM; Knizek and Grainger, 2026). The SRFM is a line-by-

line radiative transfer code that couples the Reference Forward Model (RFM) with the discrete ordinate method (DISORT) an in-house Mie code to rigorously simulate both scattering and absorption of volcanic aerosols. As shown in Fig. S3(e), the simulated top-of-atmosphere radiance spectra from the two models exhibit high consistency across different ash layer altitudes. Although minor spectral residuals (FY − SRFM) arise from the redistribution of upwelling thermal radiation by multiple scattering, these deviations remain a secondary effect compared to the massive broadband masking caused by ash absorption. The overall SO_2 absorption shape and line depths are well preserved in the FY-GeoAIR model.



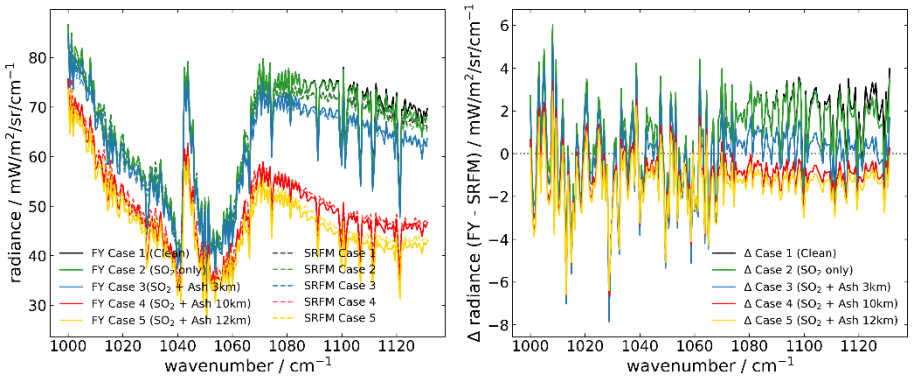


Figure S3. (a) Real and imaginary parts of the complex refractive index of volcanic ash used in the simulations. (b) Lognormal particle size distribution curves configured with different effective radii and geometric standard deviations. (c) Mass extinction coefficient and single scattering albedo calculated using Mie scattering theory. (d) Simulated top-of-atmosphere spectra (left) and the spectral residuals (right) after introducing volcanic ash (AOD = 0.2 at 10 μm) at different altitudes in the forward model. The SO_2 layer is fixed at 10 km with a column amount of 30 DU in all simulations. (e) Comparison of the simulated top-of-atmosphere radiance spectra between the FY-GeoAIR model (solid lines) and the SRFM model (dashed lines) across different atmospheric cases (left), and their corresponding spectral radiance differences (FY − SRFM) (right).

R2-M4

4. The general applicability of the proposed framework should be discussed more carefully

The manuscript suggests that the proposed framework can be directly applied to global volcanic monitoring using future geostationary hyperspectral missions.

This is an important and valuable perspective. However, the current evaluation is based on only a single volcanic eruption case.

The authors should further discuss the applicability of this framework under different conditions, including: (1) tropical versus high-latitude volcanoes; (2) explosive versus effusive eruptions; (3) low-SO_2 versus high-SO_2 emission events; (4) different surface and atmospheric backgrounds.

Additional case studies would significantly improve the robustness and general applicability of the proposed framework.

Response:

We agree with the reviewer. Since the current evaluation is based on a single case, we need to discuss the general applicability of the framework more carefully.

To address your concerns regarding applicability under different conditions, we have expanded the discussion in the Conclusion section of the revised manuscript. We explicitly pointed out the physical challenges of migrating this method to other regions: for instance, monitoring high-latitude volcanoes is limited by the weak thermal contrast over cold surfaces, which reduces the signal-to-noise ratio. Additionally, observing passive degassing events is inherently constrained by strong lower-tropospheric water vapor interference and weak signals resulting from low SO_2 loadings, which can be highly challenging.

Regarding your suggestion to provide additional validation cases, this is indeed unfeasible at the current stage, primarily due to objective observational constraints. First, as a geostationary satellite, FY-4B/GIIRS has a fixed and limited field of view. Second, because GIIRS only covers the weak SO_2 absorption band ($\nu 1$), the algorithm requires sufficiently strong SO_2 signals

to trigger effective retrievals. Within the effective observation region and operational period of GIIRS, there is currently an extreme scarcity of other eligible volcanic eruption cases with sufficiently strong signals. Therefore, we stated in the Conclusion that validating this methodology through more cases under diverse environmental conditions will be the focus of our future research.

Updated Section 6:

"With the continued deployment of geostationary hyperspectral sounders such as IRS on the European MTG satellite, GIIRS on FY-4B/C and subsequent Fengyun satellites, the GEO-driven synergistic framework developed in this study demonstrates significant potential for broader application across these different platforms. Since these emerging sensors only cover the v1 weak SO_2 absorption band, our retrieval algorithm provides a highly transferable methodological foundation across satellite platforms. Migrating this methodology to other regional geostationary platforms requires accounting for diverse volcanic and meteorological conditions. For instance, unlike the tropical explosive eruption analyzed here, monitoring high-latitude volcanoes is challenged by weak thermal contrast over cold surfaces, which reduces the signal-to-noise ratio. Observing passive degassing events is inherently limited by strong lower-tropospheric water vapor interference and weak signals from low SO_2 loadings. Therefore, future research will focus on validating this methodology through additional case studies encompassing different surface and atmospheric conditions, progressively advancing toward a coordinated global volcanic observation network."

Minor comments:

R2- Min1

1. The term "theoretical detection limit" should be clearly distinguished from an operational detection threshold.

Response:

Following your suggestion, we have distinguished between the "theoretical detection limit" and the "operational detection threshold" in the revised manuscript. In Section 4.1, we clarified that the "theoretical detection limit" (3 DU at 10 km altitude) is derived from synthetic spectral experiments considering only instrumental noise. In Section 5.2.1, we established the "operational detection threshold". Based on the statistical evaluation of real-world, SO_2-free background observations, the empirical detection limits, which inherently encompass realistic environmental interferences like clouds and water vapor, are approximately 4 DU at 15 km and 6 DU at 10 km.

R2- Min2

2. The manuscript should provide more details regarding the configuration of the radiative transfer model, including: spectral resolution; spectroscopic database; assumptions regarding surface emissivity.

Response:

Following your suggestion, we have added the requested details regarding the radiative

transfer model configuration in Section 3. Specifically, gas absorption coefficients are pre-calculated using the Line-By-Line Radiative Transfer Model (LBLRTM v12.11) based on the HITRAN database. Monochromatic radiances are simulated at 0.05 cm-1 and convolved to the instrumental resolution of 0.625 cm-1. Assumptions regarding surface emissivity are based on the UW-Madison database (Seemann et al., 2008).

Updated Section 3:

"To simulate the top-of-atmosphere radiances, gas absorption coefficients are pre-calculated using the Line-By-Line Radiative Transfer Model (LBLRTM v12.11) based on the HITRAN spectroscopic database. The forward model is driven by atmospheric profiles from European Centre for Medium-Range Weather Forecasts (ECMWF) Reanalysis v5 (ERA5) (Hersbach et al., 2020) and CAMS, alongside surface emissivity from the UW-Madison database (Seemann et al., 2008). Monochromatic radiances are simulated at a fine spectral resolution of 0.05 cm^{-1} and subsequently convolved to the instrumental resolution of 0.625 cm^{-1}."

R2- Min3

3. Some statements regarding the "global applicability" of the framework should be moderated unless additional validation cases are provided.

Response:

Following your suggestion, we agree that claiming "global applicability" based on a single validation case is not objective, and we have moderated these statements throughout the revised manuscript. In Section 6, we removed absolute claims regarding global applicability and instead objectively discussed the physical limitations the method faces when applied to other regions, such as the weak thermal contrast over high-latitude cold surfaces and the strong water vapor interference during low-altitude passive degassing events. Additionally, we explicitly stated that validating this methodology through additional case studies under diverse surface and atmospheric conditions will be the focus of our future research.

References:

Carboni, E., Grainger, R., Walker, J., Dudhia, A., and Siddans, R.: A new scheme for sulphur dioxide retrieval from IASI measurements: Application to the Eyjafjallajökull eruption of April and May 2010, Atmospheric Chemistry and Physics, 12, 11417–11434, https://doi.org/10.5194/acp-12-11417-2012, 2012.

Piontek, D., Hornby, A. J., Voigt, C., Bugliaro, L., & Gasteiger, J. (2021). Determination of complex refractive indices and optical properties of volcanic ashes in the thermal infrared based on generic petrological compositions. Journal of Volcanology and Geothermal Research, 411, 107174. https://doi.org/10.1016/j.jvolgeores.2021.107174

Reed, B. E., Peters, D. M., McPheat, R., & Grainger, R. G. (2018). The complex refractive index of volcanic ash aerosol retrieved from spectral mass extinction. Journal of Geophysical Research: Atmospheres, 123, 1339–1350. https://doi.org/10.1002/2017JD027362